The Thrust of a Collisional-Plasma Source

Amnon Fruchtman, *Senior Member, IEEE*

***Abstract*—The thrust provided by a plasma source, open at one end, is calculated for an arbitrary ratio of collision to ionization rates. If the plasma is of a low collisionality, ion pumping is dominant, and the momentum of the jet exiting the source is carried mostly by the plasma. In the collisional regime, neutrals are accelerated through charge-exchange collisions with ions, leading to neutral pumping, so that most of the momentum of the jet is carried by the neutral gas. It is shown that these ion–neutral collisions increase the thrust for a given power. However, the conventionally defined efficiency for a thruster, reflecting also the propellant utilization, is lower in the collisional regime.**

***Index Terms*—Ballistic neutrals, electric propulsion, ion-neutral collisions, plasma accelerators, plasma thrusters.**

I. Introduction

PLASMAS are used in electric propulsion employing either electric-field pressure (as in ion thrusters) or magnetic-field pressure (as in Hall thrusters) [1]. Recently, the use of plasmas in electric propulsion, which employ only their own pressure for acceleration, is being considered [2]–[18]. In our study of the thrust that can be delivered by a plasma due to its own pressure, we examined theoretically the thrust of an unmagnetized collisionless-plasma source [19] and some aspects of the thrust of a collisional-plasma source [20]. We also examined experimentally and theoretically the effect of ion-neutral collisions on the thrust in a magnetized plasma source [21], [22]. Here, we generalize these previous studies and calculate the thrust for an arbitrary plasma collisionality. We show that, as the collisionality is increased, the thrust for a given power increases, although the conventionally defined efficiency decreases.

Let us describe a reference case of cold collisionless particle beams. We consider a tube with one open end. A gas with a particle flux per unit area Γ and a velocity v_0 is ejected out of the open end. The mass of each particle is m. Since no external force is exerted on the gas, the thrust density at the open end, for example, to the right $m\Gamma v_0$, is balanced by that of particles that move to the left, carrying an opposite thrust $-m\Gamma v_0$ per unit area. If the particles that move to the left are specularly reflected at the wall, the thrust density delivered to the wall is $F = 2m\Gamma v_0$. The power deposited in the plasma is $P_T = 2m\Gamma v_0^2/2$. The mass flow rate per area unit is then $\dot{m} = 2m\Gamma$, and the ratio of thrust to power, the specific impulse

$$I_{\rm sp} \equiv \frac{F}{\dot{m}g} \tag{1}$$

(g is the free-fall acceleration), and the efficiency

$$\eta \equiv \frac{F^2}{2\dot{m}P_T} \tag{2}$$

become

$$\frac{F}{P_T} = \frac{2m\Gamma v_0}{2m\Gamma v_0^2/2} = \frac{2}{v_0} \quad I_{\rm sp} = \frac{2m\Gamma v_0}{2m\Gamma g} = \frac{v_0}{g}$$
$$\eta = \frac{(2m\Gamma v_0)^2}{2 \times 2m\Gamma \times 2m\Gamma v_0^2/2} = 1. \tag{3}$$

If the particles lose all their energies at the wall in inelastic collisions, then $F = m\Gamma v_0$, the mass flow rate per area unit is $\dot{m} = m\Gamma$, and the power is $P_T = 2m\Gamma v_0^2/2$, so that

$$\frac{F}{P_T} = \frac{m\Gamma v_0}{2m\Gamma v_0^2/2} = \frac{1}{v_0} \quad I_{\rm sp} = \frac{m\Gamma v_0}{m\Gamma g} = \frac{v_0}{g}$$
$$\eta = \frac{(m\Gamma v_0)^2}{2 \times m\Gamma \times 2m\Gamma v_0^2/2} = 0.5. \tag{4}$$

These relations exhibit what is true in general, i.e., the lower the flow velocity v_0 (and specific impulse) is, the higher the thrust for a given power is, which is the well-known tradeoff between having a large specific impulse and a large thrust. In the following analysis, we also include a finite pressure of the electrons and ion-neutral collisions and examine how the simple relations (3) and (4) are modified. The more general analysis shows that, indeed, the ion-neutral collisions that slow down the ions (and reduce the specific impulse) do result in a larger thrust for a given power, equivalently to the aforementioned relations and similarly to what we showed in [21] and [22]. Obviously, the energy required to be deposited in the plasma source is not only the kinetic energy but also the energy needed for ionization and the energy that is lost in the sheath near the back wall [19].

In Section II, we present the relations between the plasma density, Mach number, and particle flux density for arbitrary collisionality, which are the relations that we previously derived in [20]. In Section III, we write expressions for the thrust, specific impulse, and efficiency as functions of the ratio of collision to ionization rates. In Section IV, we write expressions for the collision and ionization rates as functions of the electron temperature. In Section V, we specify the neutral-gas dynamics. This allows us to write equations for the variation of the flow variables along the discharge tube. In Section VI, we derive

Manuscript received September 14, 2010; accepted October 12, 2010. Date of publication December 13, 2010; date of current version January 7, 2011. This work was supported in part by the Israel Science Foundation under Grant 864/07.

The author is with the Department of Sciences, Holon Institute of Technology, Holon 58102, Israel (e-mail: fnfrucht@hit.ac.il).

Digital Object Identifier 10.1109/TPS.2010.2089067

solutions for the equations at certain asymptotic limits. In Section VII, we present numerical examples.

II. Flow Variables

Let us consider a gas and a plasma that are contained in a long and straight tube, for example, cylindrical, where the cylinder axis lies parallel to the z-axis. There is no energy and momentum exchange with lateral walls, as collisions of the plasma with the wall are impeded by a strong axial magnetic field. A neutral gas is injected through the back wall, at $z = 0$, and neutrals and plasma flow out of the tube through one end only, located at $z = a$.

We present relations for a collisional plasma between the flow, velocity, and density that are independent of the neutral density profile, similar to those derived in [20]. We approximate the modeling of the plasma by a 1-D description. The momentum equations for the electrons and ions are

$$\frac{d\,(nT)}{dz} = -neE \quad \frac{d(mnv^2)}{dz} = neE - m\beta_c N n v. \tag{5}$$

Here, n is the density of the quasi-neutral plasma, T is the (assumed constant) electron temperature, e is the elementary charge, E is the intensity of the ambipolar electric field, m is the ion mass, v is the velocity of the plasma flow, and N is the density of the neutrals. Moreover, β_c is the rate constant of ion collisions with neutrals. We neglected the momentum transfer between electrons and heavy particles in the electron momentum equations, which is a term that we retained in [20].

Adding the two momentum equations, we obtain the standard collisional-plasma momentum equation

$$\frac{d(mnv^2 + nT)}{dz} = -m\beta_c N n v. \tag{6}$$

The continuity equation is

$$\frac{d\Gamma}{dz} = \beta N n \qquad \Gamma \equiv nv \tag{7}$$

in which $\beta = \beta(T)$ is the ionization rate constant and Γ is the plasma particle flux density. Combining the two equations, we obtain the relation

$$\frac{d(mnv^2 + nT)}{d\Gamma} = -\frac{m\beta_c}{\beta} v. \tag{8}$$

This equation can be written in the form

$$\frac{d\ln\Gamma}{dM^2} = \frac{(1 - M^2)}{2M^2\left[1 + M^2(1 + \beta_c/\beta)\right]} \tag{9}$$

in which

$$M \equiv \frac{v}{c} \tag{10}$$

is the Mach number and $c \equiv (T/m)^{1/2}$ is the ion acoustic velocity. Equation (9) shows that the flux does not grow with the velocity beyond $M = 1$. We assume that the Mach number is unity at the plasma boundaries. The equation is integrated, and the plasma flux density and plasma density are expressed as

$$\Gamma = ncM \quad n = \frac{n_0}{\left[1 + M^2(1 + \beta_c/\beta)\right]^{\frac{1}{2}\left(1 + \frac{1}{1+\beta_c/\beta}\right)}}. \tag{11}$$

Here, n_0 is the maximal plasma density (where $M = 0$). The maximal Γ and the minimal n, both at the plasma boundary, are

$$\Gamma_{\max} = n_{\min} c \quad n_{\min} = \frac{n_0}{R} \tag{12}$$

where

$$R \equiv \frac{n_0}{n_{\min}} = (2 + \beta_c/\beta)^{\frac{1}{2}\left(1 + \frac{1}{1+\beta_c/\beta}\right)}. \tag{13}$$

Note that R is a function of β_c/β only. This ratio of the maximal and minimal plasma densities is an important parameter (in [24], for example, $n_{\min}/n_0$ is denoted as g_s). The asymptotic values of R are

$$\beta_c/\beta = 0 \Longrightarrow R = 2 \quad \beta_c/\beta \gg 1 \Longrightarrow R = (\beta_c/\beta)^{1/2}. \tag{14}$$

In the next section, we turn to calculating the thrust, specific impulse, and efficiency.

III. Thrust, Specific Impulse, and Efficiency

We first calculate the potential drop across the (quasi-neutral) plasma

$$\Delta\varphi = \int_{z_0}^{a} E\,dz = -\int_{z_0}^{a} \frac{1}{ne}\frac{\partial(nT)}{\partial z}\,dz = \frac{T}{e}\ln R. \tag{15}$$

Here, z_0 is where the electric field is zero (and also $M = 0$). At the two opposite limits, we obtain

$$\begin{aligned} \beta_c/\beta = 0 &\Longrightarrow \Delta\varphi = \frac{T}{e}\ln 2 \\ \beta_c/\beta \gg 1 &\Longrightarrow \Delta\varphi = \frac{T}{e}\ln(\beta_c/\beta)^{1/2}. \end{aligned} \tag{16}$$

Note that, even if, due to nonuniform neutral-gas density, the plasma is not symmetric with respect to z_0, the potential values at both ends of the plasma are the same $\varphi(z = 0) = \varphi(z = a)$. At the back wall, there is also a voltage across the nonneutral sheath. Note also that $\Delta\varphi$, which is the maximal voltage drop across the plasma, is a function of the electron temperature and the atomic cross sections and is independent of the plasma particle flux density or the neutral-gas density. Obviously, the electron temperature itself does vary with the plasma particle flux density and the neutral-gas density.

We now calculate the thrust, the specific impulse, and the efficiency that are expected of a plasma that is used as a thruster in the simple configuration assumed here. We assume that the plasma pressure is large enough, so that it is larger than the pressure of the not-accelerated neutral gas. The thrust per unit

area is the plasma maximal pressure n_0T and can also be written as

$$F = n_0T = m\Gamma_{\max}cR. \tag{17}$$

The thrust is composed of ion, electron, and neutral-gas contributions

$$\begin{aligned} F &= F_i + F_e + F_N \quad F_e = F_i = n_{\min}T = m\Gamma_{\max}c \\ F_N &= m\Gamma_{\max}c(R-2). \end{aligned} \tag{18}$$

At the two opposite limits

$$\begin{aligned} \beta_c/\beta = 0 &\Longrightarrow F = 2m\Gamma_{\max}c = 2F_e \quad F_N = 0 \\ \beta_c/\beta \gg 1 &\Longrightarrow F = F_N = (\beta_c/\beta)^{1/2}m\Gamma_{\max}c. \end{aligned} \tag{19}$$

We note that, in the absence of a magnetic-field pressure, the only source of thrust for a plasma is its own pressure. The current-free double layer discovered in helicon sources [3] was suggested to be used for producing thrust [2]. The upstream plasma pressure is still the only source of the thrust even in the presence of the double layer [6]. The plasma pressure is then not simply expressed as in (17), however. That plasma pressure could be increased by the presence of an accelerated (by the double layer) electron beam upstream, a presence which is still debated [13], [14], [17].

We also note that, in the case of a magnetic-nozzle configuration [4], [5], [8], [12], the main contribution to the thrust is by the magnetic-field pressure. The magnetic-field pressure effectively increases the back-wall area, allowing the same plasma pressure to result in a larger force [6].

In our analysis here, we restrict ourselves to a simple form of the electron pressure and to a straight geometry. The specific impulse is

$$I_{\rm sp} = \frac{n_0T}{\dot{m}g} = \frac{c}{g}\eta_m R \tag{20}$$

where

$$\eta_m \equiv \frac{m\Gamma_{\max}}{\dot{m}} \tag{21}$$

is the propellant utilization. We assume that the velocity of the neutral gas injected from the back wall and its contribution to the thrust are negligible. At the two opposite limits

$$\begin{aligned} \beta_c/\beta = 0 &\Longrightarrow I_{\rm sp} = 2\eta_m c/g \\ \beta_c/\beta \gg 1 &\Longrightarrow I_{\rm sp} = (\beta_c/\beta)^{1/2}\eta_m c/g. \end{aligned} \tag{22}$$

In order to estimate the efficiency, we have to know how much power is deposited in the discharge. We now calculate P_E, which is the power deposited in the plasma ions due to the force by the ambipolar electric field (collisions may transfer part of that power and part of the thrust to neutrals)

$$P_E = \int_0^a nveE\,dz = 2cn_0TG = 2\Gamma_{\max}TRG \tag{23}$$

where G is defined as

$$G \equiv \left(2+\frac{\beta_c}{\beta}\right)\int_0^1 \frac{M^2}{\left[1+M^2(1+\beta_c/\beta)\right]^{\frac{1}{2}\left(3+\frac{1}{1+\beta_c/\beta}\right)}}\,dM. \tag{24}$$

Note that G is a function of the ratio β_c/β only. We used the relations $vneE = -v\partial(nT)/\partial z = -cTM(\partial n/\partial M)dM$. The same power $P_E/2$ is deposited in each of the two regions of the discharge at the two sides of the density maximum, even if the discharge is not symmetric.

At $\beta_c/\beta = 0$, the function G takes the value $G = 0.2854$, and then, G slightly increases as β_c/β increases, reaching its maximal value $G = 0.3063$ at $\beta_c/\beta = 3.52$. The function G then decreases monotonically as β_c/β increases

$$\beta_c/\beta \gg 1 \Longrightarrow G = (\beta/\beta_c)^{1/2}\left[\ln(2\sqrt{\beta_c/\beta}) - 1\right]. \tag{25}$$

The decrease is obviously slow; only at $\beta_c/\beta = 260$, the value of the function G drops to $G = 0.153$, which is half its maximal value.

The power flow carried by the electrons at each of the two plasma edges is $\Gamma_{\max}(3/2)T$. The power carried out of the plasma in the flow P_f is

$$P_f = P_E + 3\Gamma_{\max}T = \Gamma_{\max}T(2RG+3) \tag{26}$$

and is carried either by the neutrals, ions, or electrons. The total power is

$$P_T = P_f + L = \Gamma_{\max}T(2RG+3) + L. \tag{27}$$

The losses L can be written as

$$L = \Gamma_{\max}(2\varepsilon_c + \varepsilon_{\rm sh}) \tag{28}$$

where ε_c is the ionization cost per ion–electron pair and $\varepsilon_{\rm sh}$ denotes the sheath losses per ion-electron pair [23]. The losses L, which vary with T, are expected to be several tens of electronvolts per ion-electron pair and to reduce significantly the efficiency of a plasma thruster [19]. We are not addressing here this issue of losses.

At the two opposite limits

$$\begin{aligned} \beta_c/\beta = 0 &\Longrightarrow P_E = 1.141\,6\Gamma_{\max}T \\ &\qquad\quad P_f = 4.141\,6\Gamma_{\max}T \\ \beta_c/\beta \gg 1 &\Longrightarrow P_E = 2\Gamma_{\max}T\left[\ln\left(2\sqrt{\beta_c/\beta}\right) - 1\right] \\ &\qquad\quad P_f = \Gamma_{\max}T\left[2\ln\left(2\sqrt{\beta_c/\beta}\right) + 1\right]. \end{aligned} \tag{29}$$

At the collisionless limit $\beta_c/\beta = 0$, we may express P_E alternatively as the kinetic energy carried by the ions exiting the discharge instead of as the calculated work per unit time on the ions by the ambipolar electric field, as in (23). The power would then be $P_E = 2m\Gamma_{\max}c^2/2 = \Gamma_{\max}T$ and is somewhat different than the value obtained in (29), reflecting the inconsistency of the assumption of zero ion temperature for an ionizing plasma.

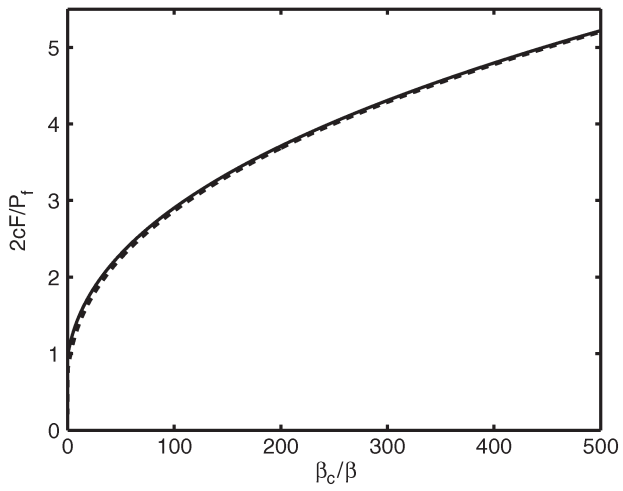

Fig. 1. (Solid line) Dimensionless thrust over power $2cF/P_f$ ($= 2cF/P_T$ for $L = 0$) as a function of the ratio β_c/β, according to (30). (Dashed line) Also shown is this quantity calculated by the approximated expression that holds for $\beta_c/\beta \gg 1$ (31).

The ratio of thrust to power is

$$\frac{F}{P_T} = \frac{1}{2c\left\{G + \left[1.5 + L/(2\Gamma_{\max}T)\right]/R\right\}}. \tag{30}$$

At the two opposite limits

$$\begin{aligned}
&\beta_c/\beta = 0 \\
&\quad \Longrightarrow \frac{F}{P_T} = \frac{1}{2c\left[1.0354 + L/(4\Gamma_{\max}T)\right]} \\
&\beta_c/\beta \gg 1 \\
&\quad \Longrightarrow \frac{F}{P_T} = \frac{1}{2c(\beta/\beta_c)^{1/2}\left[\ln\left(2\sqrt{\beta_c/\beta}\right) + 0.5 + L/(2\Gamma_{\max}T)\right]}.
\end{aligned} \tag{31}$$

If the kinetic energy of the ions is used in the calculation, as explained earlier, 1.0354 is replaced by unity.

Fig. 1 shows $2cF/P_f$ ($= 2cF/P_T$ for $L = 0$) as a function of the ratio β_c/β, according to (30). It can be seen in the figure that this dimensionless thrust over power increases as the collisionality is increased. Also shown in the figure is this quantity calculated by the approximated expression that holds for $\beta_c/\beta \gg 1$ (31).

The efficiency is expressed as $\eta = (g/2)I_{\rm sp}F/P_T$, and therefore

$$\eta = \frac{\eta_m R}{4\left\{G + \left[1.5 + L/(2\Gamma_{\max}T)\right]/R\right\}}. \tag{32}$$

At the two opposite limits

$$\begin{aligned}
&\beta_c/\beta = 0 \Longrightarrow \eta = \frac{\eta_m}{2\left[1.0354 + L/(4\Gamma_{\max}T)\right]} \\
&\beta_c/\beta \gg 1 \Longrightarrow \eta = \frac{\eta_m}{4(\beta/\beta_c)\left[\ln\left(2\sqrt{\beta_c/\beta}\right) + 0.5 + L/(2\Gamma_{\max}T)\right]}.
\end{aligned} \tag{33}$$

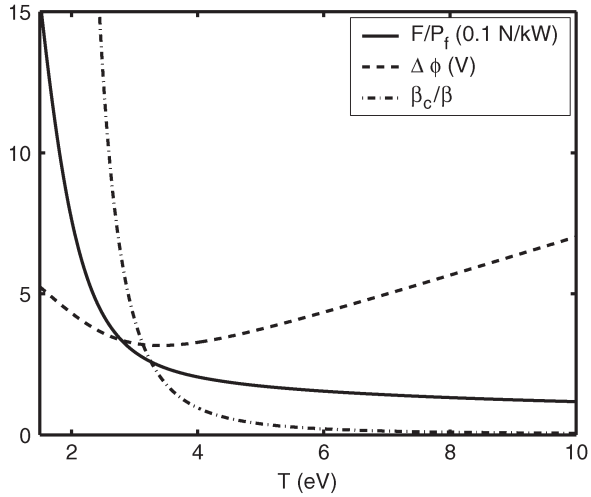

Fig. 2. Variations as functions of T for an argon plasma of β_c/β [according to (34) and (35)], F/P_f [according to (30) with $L = 0$] in 0.1 N/kW, and $\Delta\varphi$ [according to (15)] in volts.

For a given propellant utilization η_m, the ionization increases with an increase of the collisionality β_c/β. However, as we show hereinafter, η_m is expected to decrease when the collisionality is increased, resulting in a lower efficiency for a higher collisionality.

IV. Variation With the Electron Temperature

We now calculate how F/P_f and $\Delta\varphi$ vary with the electron temperature T for an argon plasma. For that, we specify the dependence of β_c/β on T. We take the ion-neutral collision rate constant as [23]

$$\beta_c = 8.99 \times 10^{-16}\left(\frac{\alpha_R}{A_R}\right)^{1/2} \text{m}^3/\text{s} \tag{34}$$

where A_R is the reduced mass in atomic mass units and α_R is the relative polarizability. In our case, in which ions and neutrals are of the same mass, $A_R = A/2$. The ionization rate constant, when the electron distribution is Maxwellian, is

$$\beta = \sigma_0 v_{te}\exp\left(-\frac{\epsilon_i}{T}\right) \tag{35}$$

where $v_{te} \equiv (8T/\pi m_e)^{1/2}$ is the electron thermal velocity and $\sigma_0 \equiv \pi(e^2/4\pi\epsilon_0\epsilon_i)^2$, with ϵ_0 being the permittivity of the vacuum and ϵ_i being the ionization energy. Equation (35) is an approximated form, for $T \ll \epsilon_i$, of the rate constant given in [23]. In our example of an argon discharge, $A = 40$, $\epsilon_i = 15.6$ eV, and $\alpha_R = 11.1$.

Fig. 2 shows several quantities as functions of T for an argon plasma. These are β_c/β [according to (34) and (35)], F/P_f [according to (30) with $L = 0$], and $\Delta\varphi$ [according to (15)].

V. Neutral Pumping

In order to calculate the efficiencies, we need to solve self-consistently for the dynamics of the plasma and neutral gas. We assume that the neutrals are injected through the wall at $z = 0$ and move ballistically to the right (positive z), all with the same

constant slow velocity v_a. Since some of these slow ballistic neutrals are ionized or being accelerated through collisions with fast ions, their flux density $\Gamma_s(z)$ and density $N_s(z)$ vary along the source. We assume, however, that neutrals, which were not ionized or accelerated by collisions, maintain their velocity, so that the relation $v_a = \Gamma_s(z)/N_s(z)$ holds. Some of the neutrals are accelerated through charge-exchange collisions with fast ions, leaving quickly the system, either to the right or to the left, in the direction of the plasma flow. In [20], we made a distinction between this process of depleting neutrals through their collisions with ions, which we called neutral pumping, and the process of depleting neutrals through ionization, which we called ion pumping. The fast component of the neutral flow, resulting from these charge-exchange collisions, is of a flux density $\Gamma_f(z)$ and density $N_f(z)$. Particle conservation is expressed as

$$\Gamma + \Gamma_s + \Gamma_f = \frac{\dot{m}}{m} \tag{36}$$

where $\dot{m}$ is the mass flow rate per area unit, and the total neutral-gas density is

$$N = N_s + N_f. \tag{37}$$

The continuity equations for the various species are

$$\frac{d\Gamma}{dz} = \beta(N_s + N_f)n \quad \frac{d\Gamma_s}{dz} = -\beta N_s n - \beta_c N_s n \tag{38}$$

$$\frac{d\Gamma_f}{dz} = \beta_c N_s n - \beta N_f n. \tag{39}$$

We assume that the residence time of the fast neutral-gas particles is much shorter than that of the slow neutrals. The density of the fast neutral-gas particles is then much lower than the density of the slow neutral-gas particles so that

$$N_f \ll N_s \quad N \cong N_s. \tag{40}$$

Because of their short residence time, we also assume that the ionization of the fast neutrals is negligible. The continuity equations are then approximated as

$$\frac{d\Gamma}{dz} = \beta N_s n \quad \frac{d\Gamma_s}{dz} = -(\beta + \beta_c)N_s n$$

$$\frac{d\Gamma_f}{dz} = \beta_c N_s n. \tag{41}$$

From here, we obtain the relation

$$\Gamma_f = \frac{\beta_c}{\beta}\Gamma \tag{42}$$

and therefore, (36) becomes

$$\left(1 + \frac{\beta_c}{\beta}\right)\Gamma + N v_a = \frac{\dot{m}}{m}. \tag{43}$$

This way, we express the varying neutral-gas density $N(z)$ as a function of the varying plasma particle flux density $\Gamma(z)$.

We now combine the equations for the plasma with the expression for the neutral-gas density. We first express the left-hand side of (6) in terms of variables M and Γ ($n = \Gamma/cM$)

$$\Gamma\left(1 - \frac{1}{M^2}\right)\frac{dM}{dz} + \left(M + \frac{1}{M}\right)\frac{d\Gamma}{dz} = -\frac{\beta_c}{c}N\Gamma.$$

We then express $d\Gamma/dz$ with the right-hand side of the continuity equation (7). Finally, we employ (43) to write an expression for N, in which, for Γ, following (11) and (12), we use the expression $\Gamma = \Gamma_{\max} RM/[1 + M^2(1 + \beta_c/\beta)]^{(1/2)(1+(1/(1+\beta_c/\beta)))}$. The resulting governing equation, which is an equation for the plasma Mach number, is

$$(1-M^2)\frac{dM}{d\xi} = \frac{\beta}{c}Q\left[1 - \eta_{mc}\frac{RM}{[1+M^2(1+\beta_c/\beta)]^{\frac{1}{2}\left(1+\frac{1}{1+\beta_c/\beta}\right)}}\right] \times \left[M^2\left(1 + \frac{\beta_c}{\beta}\right) + 1\right] \tag{44}$$

where

$$\xi \equiv \frac{z}{a} \qquad Q \equiv \frac{\dot{m}}{m}\tau_N \qquad \tau_N \equiv \frac{a}{v_a} \tag{45}$$

with τ_N being the transit time of the slow neutral-gas particles, and

$$\eta_{mc} \equiv \left(1 + \frac{\beta_c}{\beta}\right)\eta_m \leq 1. \tag{46}$$

Note that η_m is always smaller than unity when $\beta_c \neq 0$. The appropriate propellant utilization is η_{mc} that expresses also neutral pumping. The boundary conditions are

$$M(\xi = 0) = -1 \quad M(\xi = 1) = 1. \tag{47}$$

Using these boundary conditions, we write the solution for (44) as (48), shown at the bottom of the next page, with the solvability condition given in (49), also shown at the bottom of the next page. In addition to (49), we use the energy balance equation (26) to write

$$\eta_{mc} = \left(1 + \frac{\beta_c}{\beta}\right)\frac{H}{T\,(2RG + 3)} \tag{50}$$

where

$$H = \frac{P_f}{\dot{m}/m} \tag{51}$$

is the power deposited in the flow per particle. Before we turn to numerical examples, let us discuss some asymptotic limits.

VI. Asymptotic Limits

We present three asymptotic limits: low neutral-gas depletion, collisionless plasma, and highly collisional plasma.

A. Uniform Neutral-Gas Density

Let us assume that the neutral-gas density is uniform $N = \dot{m}/(mv_a)$. We substitute $\eta_{mc} = 0$ in (48) and (49). The solution becomes [24]

$$(2+\beta_c/\beta)\arctan\left[M(1+\beta_c/\beta)^{1/2}\right] - M(1+\beta_c/\beta)^{1/2} = (1+\beta_c/\beta)^{3/2}\frac{\beta Q}{c}\left(\xi-\frac{1}{2}\right) \quad (52)$$

where

$$(2+\beta_c/\beta)\arctan\left[(1+\beta_c/\beta)^{1/2}\right] - (1+\beta_c/\beta)^{1/2} = (1+\beta_c/\beta)^{3/2}\frac{\beta Q}{2c}. \quad (53)$$

At the two opposite limits, we recover the linear collisionless and diffusion cases

$$\beta_c/\beta = 0 \Longrightarrow \frac{\pi}{2} - 1 = \frac{\beta Q}{2c}$$
$$\beta_c/\beta \gg 1 \Longrightarrow \frac{\pi}{2} = (\beta\beta_c)^{1/2}\frac{Q}{2c}. \quad (54)$$

B. Collisionless Case

We now allow neutral-gas depletion so that N is not uniform. We first examine the collisionless case $\beta_c = 0$ so that $\eta_{mc} = \eta_m$. Equations (48) and (49) become

$$-1-M-\eta_m\ln\left(\frac{M^2+1-2\eta_m M}{2+2\eta_m}\right) + 2\sqrt{1-\eta_m^2}\left[\arctan\left(\frac{M-\eta_m}{\sqrt{1-\eta_m^2}}\right)-\arctan\left(\frac{-1-\eta_m}{\sqrt{1-\eta_m^2}}\right)\right] = \frac{\beta}{c}Q\xi \quad (55)$$

and

$$-2-\eta_m\ln\left(\frac{1-\eta_m}{1+\eta_m}\right) + 2\sqrt{1-\eta_m^2}\left[\arctan\left(\frac{1-\eta_m}{\sqrt{1-\eta_m^2}}\right)-\arctan\left(\frac{-1-\eta_m}{\sqrt{1-\eta_m^2}}\right)\right] = \frac{\beta}{c}Q. \quad (56)$$

Equations (55) and (56) were presented in [19]. Note that the equations at the linear collisionless limit presented in Section VI-A are recovered if $\eta_m = 0$ is substituted in (55) and (56).

We add the power balance (50) approximated in the collisionless limit by using $\eta_m = \eta_{mc}$, $R = 2$, and $G = 0.2854$, as explained earlier. The approximated power balance therefore becomes

$$\eta_m = \frac{H}{4.141\,6T}. \quad (57)$$

C. High-Collisionality Case

As in Section VI-B, we allow neutral-gas depletion so that N is not uniform, but here, we examine the opposite limit of high collisionality $\beta_c/\beta \gg 1$ in which neutral pumping described earlier is dominant. We repeat here the analysis of this case presented in [20]. We assume that $1 - M^2 \ll 1$, approximate the plasma particle flux density as $\Gamma = cMn_0/\sqrt{1+M^2(\beta_c/\beta)}$, and define $\Gamma_n \equiv (\Gamma/n_0 c)(\beta_c/\beta)^{1/2}$. We then change the variable of integration in (48) and (49) from M to Γ_n. The equations are integrated to

$$\frac{\Gamma_n - \eta_{mc}}{\sqrt{1-\Gamma_n^2}\sqrt{1-\eta_{mc}^2}} = \cot\left[\pi(1-\xi)\right] \quad (58)$$

with the solvability condition

$$\frac{\beta}{c}Q = \left(\frac{\beta}{\beta_c}\right)^{1/2}\frac{\pi}{(1-\eta_{mc}^2)^{1/2}}. \quad (59)$$

Equations (58) and (59) were presented in [20]. Note that the linear diffusion limit of Section VI-A is recovered by substituting $\eta_{mc} = 0$ in (58) and (59).

$$\int_{-1}^{M}\frac{(1-M'^2)dM'}{\left[M'^2(1+\beta_c/\beta)+1\right]\left\{1-\eta_{mc}R\left[1+M'^2(1+\beta_c/\beta)\right]^{-\frac{1}{2}\left(1+\frac{1}{1+\beta_c/\beta}\right)}M'\right\}} = \frac{\beta}{c}Q\xi \quad (48)$$

$$\int_{-1}^{1}\frac{(1-M^2)dM}{\left[M^2(1+\beta_c/\beta)+1\right]\left\{1-\eta_{mc}R\left[1+M^2(1+\beta_c/\beta)\right]^{-\frac{1}{2}\left(1+\frac{1}{1+\beta_c/\beta}\right)}M\right\}} = \frac{\beta}{c}Q \quad (49)$$

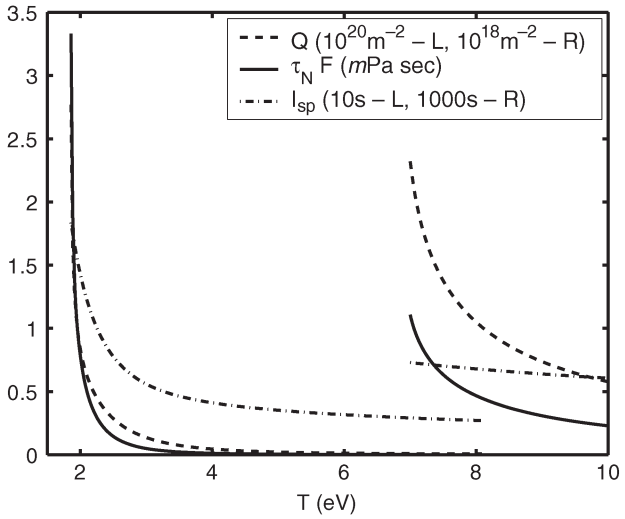

Fig. 3. Variation with T. The three curves on the right side are for $H = 25$ eV/particle (low collisionality). The three curves on the left side are for $H = 0.1$ eV/particle (high collisionality). The gas is argon. The "R" and "L" in the units in the legend refer to the curves on the right and left, respectively.

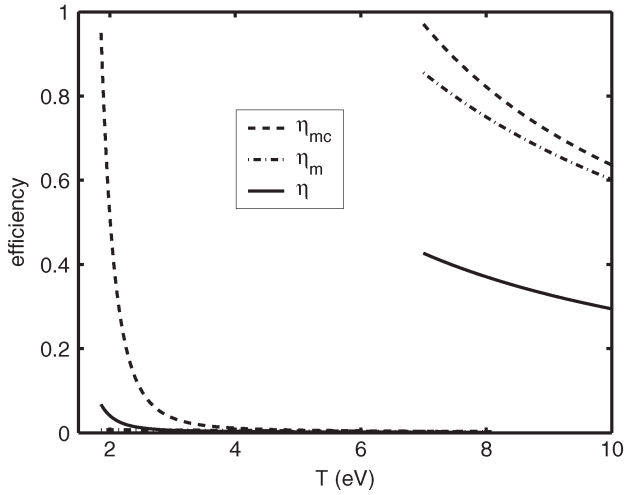

Fig. 4. Efficiencies as functions of T. The ionization and sheath losses at the back wall are neglected [$L = 0$ in (32)]. The three curves on the right side are for $H = 25$ eV/particle (low collisionality). The three curves on the left side are for $H = 0.1$ eV/particle (high collisionality). The gas is argon.

We add here the power balance, which is the approximated form of (50)

$$\eta_{mc} = \frac{\beta_c}{\beta} \frac{H}{T\left[2\ln\left(2\sqrt{\beta_c/\beta}\right) + 1\right]}. \tag{60}$$

In this neutral pumping limit $\beta_c/\beta \gg 1$, we express the specific impulse as

$$I_{\rm sp} = \frac{2c}{g}\eta_{mc}(\beta/\beta_c)^{1/2} \tag{61}$$

and the efficiency as

$$\eta = \frac{\eta_{mc}}{4\left[\ln\left(2\sqrt{\beta_c/\beta}\right) + 0.5 + L/(2\Gamma_{\max}T)\right]}. \tag{62}$$

At the limit where $\eta_{mc} \simeq 1$, the specific impulse and the efficiency decrease with the increase of the collisionality β_c/β.

In the next section, we turn to numerical examples.

VII. Numerical Examples

We specify H and Q and solve (49) and (50) for argon to find η_{mc} and T. In the examples here, H takes two values: 0.1 and 25 eV/particle. The normalized gas flow rate Q was varied continuously in the calculation. We chose to show the variables as a function of T on the horizontal axis in Figs. 3 and 4. Fig. 3 therefore shows Q as a function of T for argon (the dependence of β_c/β on T is shown in Fig. 2). Also shown in Fig. 3 are $\tau_N F = mQc\eta_m R$ [calculated by using (17) and (21)] and $I_{\rm sp} = c\eta_m R/g$. For evaluating these expressions, we calculate the propellant utilization as $\eta_m = \eta_{mc}/(1 + \beta_c/\beta)$. Note that $\tau_N F$ is in units of impulse per unit area (which are used to measure a dynamic viscosity). However, $\tau_N F$ represents the thrust density (which is in units of pressure), and for specified τ_N and cross-sectional area of the tube, $\tau_N F$ represents the thrust itself. The three curves on the right side of the figure are for $H = 25$ eV/particle. Since $\beta_c/\beta \ll 1$ for those values of T, these curves describe the behavior near the collisionless limit. The three curves on the left side of the figure are for $H = 0.1$ eV/particle, and they mostly describe the behavior in the collisional regime. It can be seen in the figure that $I_{\rm sp}$ is much larger in the collisionless case, while $\tau_N F$ is considerably larger in the collisional case.

Fig. 4 shows the efficiencies η_{mc}, η_m, and η as functions of T for the same two values of H mentioned previously. Since, near the collisionless limit (the three curves on the right side of the figure), ionization (ion pumping) is dominant over the charge-exchange collisions, η_{mc} and η_m are of a similar value. The highest calculated efficiency is close to 0.5, which is the maximal possible value, as shown in the Introduction. In the collisional case (the three curves on the left side of Fig. 4), the efficiency η_{mc} almost reaches unity at a low T while η_m is still very low since charge-exchange collisions are dominant over ionization. Neutral pumping is the dominant process here. The efficiency η [according to (32) with $L = 0$] is very low. Figs. 3 and 4 show that the thrust for a given power is larger in a collisional plasma while the conventionally defined efficiency is higher for a low-collisionality plasma. We note that taking a realistic finite value for L, expressing ionization cost and sheath losses, should make the efficiency considerably lower [19].

Figs. 5–8 show the profiles of densities and thrust in low-collisionality (Figs. 5 and 7) and high-collisionality (Figs. 6 and 8) argon plasmas. In Figs. 5 and 7, $H = 25$ eV/particle, and $Q = 2.32 \times 10^{18}$ m^{-2}, resulting in $T = 7$ eV, $\beta_c/\beta = 0.1351$, $c = 4094$ m/s, $\eta_{mc} = 0.9709$, $\eta_m = 0.8553$, and $\eta = 0.4266$. Also, $\tau_N F = 1.108$ mPa $\cdot$ s, and $F/P_f = 0.1197$ N/kW. Note that $F/P_f \cong 1/(2.07c)$ according to the first equation in (31).

In Figs. 6 and 8, $H = 0.1$ eV/particle, and $Q = 2.77 \times 10^{20}$ m^{-2}, resulting in $T = 1.86$ eV, $\beta_c/\beta = 128.9$, $c = 2110$ m/s, $\eta_{mc} = 0.9499$, $\eta_m = 0.0073$, and $\eta = 0.0676$. Also, $\tau_N F = 3.329$ mPa $\cdot$ s, and $F/P_f = 0.7515$ N/kW. It is easily verified that F/P_f satisfies the second equation in (31).

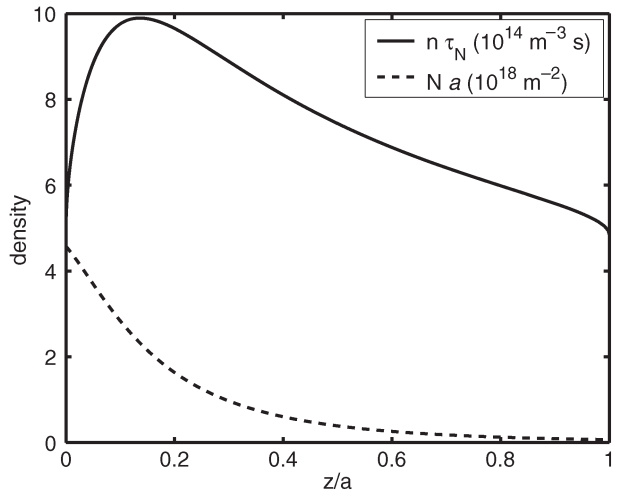

Fig. 5. Profiles of the normalized plasma and neutral-gas densities in argon for the low-collisionality case of $H = 25$ eV/particle and $Q = 2.32 \times 10^{18}$ m^{-2} (resulting in $T = 7$ eV, $\beta_c/\beta = 0.1351$, $c = 4094$ m/s, $\eta_{mc} = 0.9709$, $\eta_m = 0.8553$, and $\eta = 0.4266$). The gas inlet is on the left, and the exit, which is the open boundary, is on the right.

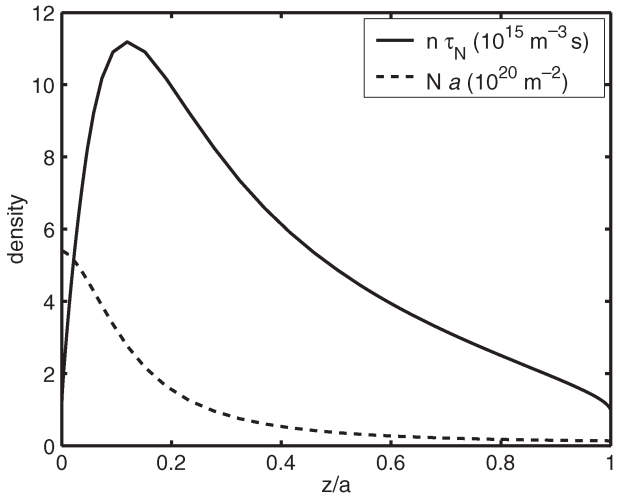

Fig. 6. Profiles of the normalized plasma and neutral-gas densities in argon for the high-collisionality case of $H = 0.1$ eV/particle and $Q = 2.77 \times 10^{20}$ m^{-2} (resulting in $T = 1.86$ eV, $\beta_c/\beta = 128.9$, $c = 2110$ m/s, $\eta_{mc} = 0.9499$, $\eta_m = 0.0073$, and $\eta = 0.0676$). The gas inlet is on the left, and the exit, which is the open boundary, is on the right.

The two examples were chosen at the low temperature edge of the two sets of curves in Figs. 3 and 4; in both examples, η_{mc} is close to unity. It is clear also from these examples that $\tau_N F$ and F/P_f are considerably larger while the efficiency is much lower in the high-collisionality case.

Using (11), (17), (21), and (45), we write $n\tau_N$, which is proportional to the plasma density, as

$$n\tau_N = \frac{Q\eta_m R}{c\left[1 + M^2\left(1 + \beta_c/\beta\right)\right]^{\frac{1}{2}\left(1+\frac{1}{1+\beta_c/\beta}\right)}}. \tag{63}$$

Similarly, using also (43), we write Na, which is proportional to the neutral-gas density, as

$$Na = Q\left\{1 - \frac{\eta_{mc} RM}{\left[1 + M^2\left(1 + \beta_c/\beta\right)\right]^{\frac{1}{2}\left(1+\frac{1}{1+\beta_c/\beta}\right)}}\right\}. \tag{64}$$

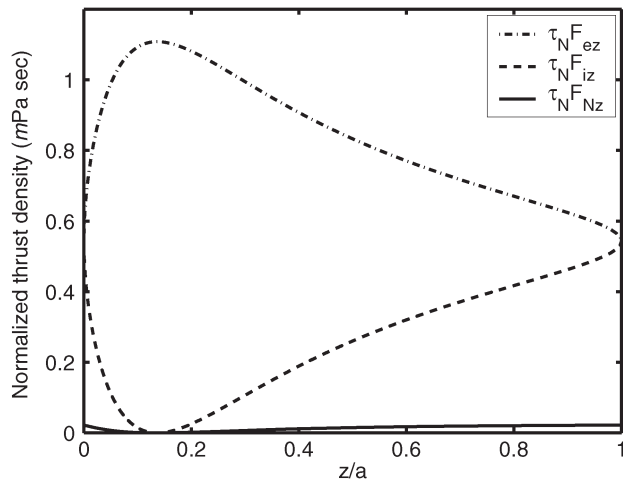

Fig. 7. Profiles of the normalized thrust densities of the electrons, ions, and neutrals in argon for the low-collisionality case of the same parameters as in Fig. 5: $H = 25$ eV/particle and $Q = 2.32 \times 10^{18}$ m^{-2} (resulting in $T = 7$ eV, $\beta_c/\beta = 0.1351$, $c = 4094$ m/s, $\eta_{mc} = 0.9709$, $\eta_m = 0.8553$, and $\eta = 0.4266$). The units are of impulse density (in millipascal seconds). The gas inlet is on the left, and the exit, which is the open boundary, is on the right. At the boundaries, most of the momentum is carried by the plasma.

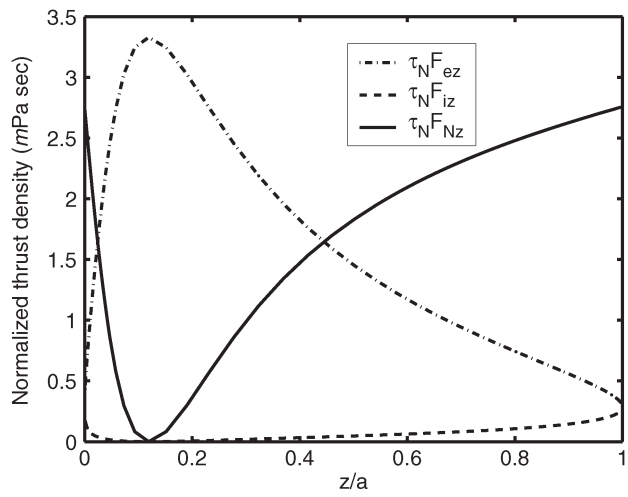

Fig. 8. Profiles of the normalized thrust densities of the electrons, ions, and neutrals in argon for the high-collisionality case of the same parameters as in Fig. 6: $H = 0.1$ eV/particle and $Q = 2.77 \times 10^{20}$ m^{-2} (resulting in $T = 1.86$ eV, $\beta_c/\beta = 128.9$, $c = 2110$ m/s, $\eta_{mc} = 0.9499$, $\eta_m = 0.0073$, and $\eta = 0.0676$). The units are of impulse density (in millipascal seconds). The gas inlet is on the left, and the exit, which is the open boundary, is on the right. At the boundaries, most of the momentum is carried by the neutral gas.

Note that the maximal and minimal values of Na are $Q(1 + \eta_{mc})$ (at the back wall) and $Q(1 - \eta_{mc})$ (at the exit) for any value of β_c/β. The maximal value of $n\tau_N$ is $2Q\eta_m/c$ for a collisionless plasma ($\beta_c/\beta = 0$) and $Q\eta_m(\beta_c/\beta)^{1/2}/c$ for a collisional plasma ($\beta_c/\beta \gg 1$). The minimal value of $n\tau_N$ is $Q\eta_m/c$ for any value of β_c/β.

Figs. 7 and 8 show the momentum along the discharge, for the same set of parameters as in Figs. 5 and 6, respectively. We use again (11) and (17) to express $\tau_N F_{ez}$, which is in units of impulse per unit area but is proportional to the electron pressure $F_{ez} = nT$, as

$$\tau_N F_{ez} = \tau_N F \frac{1}{\left[1 + M^2\left(1 + \beta_c/\beta\right)\right]^{\frac{1}{2}\left(1+\frac{1}{1+\beta_c/\beta}\right)}} \tag{65}$$

where $\tau_N F = mQc\eta_m R$, as before. The normalized ion thrust density $\tau_N F_{iz}$ (τ_N multiplied by the ion thrust density $F_{iz} = m\Gamma v$) is

$$\tau_N F_{iz} = \tau_N F \frac{M^2}{\left[1 + M^2\left(1 + \beta_c/\beta\right)\right]^{\frac{1}{2}\left(1+\frac{1}{1+\beta_c/\beta}\right)}} \tag{66}$$

while the normalized neutral-gas thrust density $\tau_N F_{Nz}$ (τ_N multiplied by the neutral-gas thrust density $F_{Nz} = n_0 T - F_{ez} - F_{iz}$) is

$$\tau_N F_{Nz} = \tau_N F \left\{ 1 - \frac{1 + M^2}{\left[1 + M^2(1 + \beta_c/\beta)\right]^{\frac{1}{2}\left(1+\frac{1}{1+\beta_c/\beta}\right)}} \right\}. \tag{67}$$

The normalized thrust densities represent the relative contributions of the electrons, ions, and neutrals to the momentum of the jet and to the thrust. As shown in Figs. 7 and 8, in both low- and high-collisionality plasmas, at the peak of the plasma density, the total pressure is equal to the electron pressure (within the model here), while the ion and neutral momenta are zero there. At each of the tube ends, however, the ion contribution to the thrust becomes equal to the electron contribution. In the low-collisionality case, the sum of the electron and ion momenta nearly equals the total pressure. In the collisional case, this sum is small, and most of the momentum is carried by the neutral gas.

Once τ_N is specified, in addition to Q, the particle flow rate density $\dot{m}/m$ is determined. Let us assume that $\tau_N = 10^{-3}$ s. In the low-collisionality case shown in Figs. 5 and 7, the particle flow rate density turns out to be then $\dot{m}/m = 2.32 \times 10^{21}$ m$^{-2} \cdot$ s^{-1}, while in the collisional case shown in Figs. 6 and 8, it is $\dot{m}/m = 2.77 \times 10^{23}$ m$^{-2} \cdot$ s^{-1}. The power density (for $L = 0$) $P_f = H\dot{m}/m$ is determined as $P_f = 9280$ W $\cdot$ m^{-2} in the low-collisionality case and as $P_f = 4430$ W $\cdot$ m^{-2} in the collisional case. The maximal plasma density turns out to be, according to (63), $n_{\max} = [Q\eta_m/(c\tau_N)](2 + \beta_c/\beta)^{(1/2)(1+(1/(1+\beta_c/\beta)))}$. Therefore, in the numerical example of the low-collisionality case, $n_{\max} = 9.89 \times 10^{17}$ m^{-3}, while in the numerical example of the collisional case, $n_{\max} = 1.12 \times 10^{19}$ m^{-3}. The pressure (thrust density) is $F = 1.108$ Pa in the low-collisionality case and is 3.329 Pa in the collisional case.

If we further choose the tube length to be $a = 0.2$ m (corresponding to $v_a = 200$ m $\cdot$ s^{-1}), the maximal and minimal neutral-gas densities are, according to (64), $N_{\max} = (Q/a)(1 + \eta_{mc})$ and $N_{\min} = (Q/a)(1 - \eta_{mc})$. Therefore, in the low-collisionality example given here ($H = 25$ eV/particle and $Q = 2.32 \times 10^{18}$ m^{-2}), the neutral-gas density varies between $N_{\max} = 2.29 \times 10^{19}$ m^{-3} and $N_{\min} = 3.38 \times 10^{17}$ m^{-3}, while in the collisional example ($H = 0.1$ eV/particle and $Q = 2.77 \times 10^{20}$ m^{-2}), the neutral-gas density varies between $N_{\max} = 2.70 \times 10^{21}$ m^{-3} and $N_{\min} = 6.93 \times 10^{19}$ m^{-3}.

Let us now specify the cross-sectional area of the plasma source as, for example, 10^{-2} m^2. In the low-collisionality case, the thrust (the pressure multiplied by that area) is 0.0111 N, and the deposited power (for $L = 0$) is 92.8 W. In the collisional case, the thrust turns out to be 0.0333 N, and the deposited power (for $L = 0$) is 44.3 W.

VIII. Summary

We have analyzed the performance as a thruster of a plasma source that uses only its own pressure for acceleration. The source was assumed to have a constant cross section with no nozzle effects, and we allowed an arbitrary plasma collisionality. We have shown that, as the collisionality is increased, the thrust for a given power increases, although the conventionally defined efficiency, reflecting also the propellant utilization, decreases. The collisional regime might be advantageous in the cases that propellant saving is not a major concern, such as perhaps for air-breathing propulsion [25].

As mentioned before, in the estimate of the power deposited, we only considered the power deposited in the ion acceleration. Ionization and back-wall losses are usually large. If also included in the calculation, these losses are expected to result in a considerably lower calculated efficiency. On the other hand, once the simplifying assumption of a uniform electron temperature is removed, it is likely to result in a higher efficiency. The assumption of a uniform electron temperature made here is one possible reason for the lower efficiency found here than in [11]. The assumption that the fast neutral-gas particles that result from charge-exchange collisions do not experience either ionizations or further charge-exchange collisions also results in the underestimation of the efficiency. In a future analysis, these simplifying assumptions will be relaxed.

Acknowledgment

The author would like to thank Prof. N. J. Fisch, Dr. Y. Raitses, G. Makrinich, and Dr. D. Zoler for the helpful comments.

References

[1] M. Martinez-Sanchez and J. E. Pollard, "Spacecraft electric propulsion—An overview," *J. Propul. Power*, vol. 14, no. 5, pp. 688–699, Sep./Oct. 1998.

[2] C. Charles, "Plasmas for spacecraft propulsion," *J. Phys. D, Appl. Phys.*, vol. 42, no. 16, pp. 163 001-1–163 001-18, Aug. 2009.

[3] C. Charles, "A review of recent laboratory double layer experiments," *Plasma Sources Sci. Technol.*, vol. 16, no. 4, pp. R1–R25, Nov. 2007.

[4] F. F. Chang-Diaz, "The Vasimir rocket," *Sci. Amer.*, vol. 283, no. 5, pp. 72–79, 2000.

[5] W. M. Manheimer and R. F. Fernsler, "Plasma acceleration by area expansion," *IEEE Trans. Plasma Sci.*, vol. 29, no. 1, pp. 75–84, Feb. 2001.

[6] A. Fruchtman, "Electric field in a double layer and the imparted momentum," *Phys. Rev. Lett.*, vol. 96, no. 6, pp. 065 002-1–065 002-4, Feb. 2006.

[7] A. Dunaevsky, Y. Raitses, and N. J. Fisch, "Plasma acceleration from radio-frequency discharge in dielectric capillary," *Appl. Phys. Lett.*, vol. 88, no. 25, pp. 251 502-1–251 502-3, Jun. 2006.

[8] R. Winglee, T. Ziemba, L. Giersch, J. Prager, J. Carscadden, and B. R. Roberson, "Simulation and laboratory validation of magnetic nozzle effects for the high power helicon thruster," *Phys. Plasmas*, vol. 14, no. 6, pp. 063 501-1–063 501-14, Jun. 2007.

[9] F. F. Chen, "Permanent magnet helicon source for ion propulsion," *IEEE Trans. Plasma Sci.*, vol. 36, pt. 1, no. 5, pp. 2095–2110, Oct. 2008.

[10] D. Pavarin, F. Ferri, M. Manente, D. Curreli, Y. Guclu, D. Melazzi, D. Rondini, S. Suman, J. Carlsson, C. Bramanti, E. Ahedo, V. Lancellotti, K. Katsonis, and G. Markelov, "Design of 50 W helicon plasma thruster," presented at the 31st Int. Electric Propulsion Conf., Ann Arbor, MI, Sep. 20–24, 2009, IEPC Paper 2009-205.

[11] O. Batishchev, "Minihelicon plasma thruster," *IEEE Trans. Plasma Sci.*, vol. 37, no. 8, pp. 1563–1571, Aug. 2009.
[12] P. F. Schmit and N. J. Fisch, "Magnetic detachment and plume control in escaping magnetized plasma," *J. Plasma Phys.*, vol. 75, pt. 3, pp. 359–371, Jun. 2009.
[13] A. Aanesland, C. Charles, M. A. Lieberman, and R. W. Boswell, "Upstream ionization instability associated with a current-free double layer," *Phys. Rev. Lett.*, vol. 97, no. 7, pp. 075 003-1–075 003-4, Aug. 2006.
[14] K. Takahashi, C. Charles, R. W. Boswell, T. Kaneko, and R. Hatakeyama, "Measurement of the energy distribution of trapped and free electrons in a current-free double layer," *Phys. Plasmas*, vol. 14, no. 11, pp. 114 503-1–114 503-4, Nov. 2007.
[15] C. M. Denning, M. Wiebold, and J. E. Scharer, "Observation of neutral depletion and plasma acceleration in a flowing high-power argon helicon plasma," *Phys. Plasmas*, vol. 15, no. 7, pp. 072 115-1–072 115-12, Jul. 2008.
[16] S. Shinohara, T. Hada, T. Motomura, K. Tanaka, T. Tanikawa, K. Toki, Y. Tanaka, and K. P. Shamrai, "Development of high-density helicon plasma sources and their applications," *Phys. Plasmas*, vol. 16, pp. 057104-1–057104-10, 2009.
[17] S. Chakraborty Thakur, A. Hansen, and E. E. Scime, "Threshold for formation of a stable double layer in an expanding helicon plasma," *Plasma Sources Sci. Technol.*, vol. 19, no. 2, pp. 025 008-1–025 008-10, Apr. 2010.
[18] A. W. Kieckhafer and M. L. R. Walker, "RF power system for thrust measurements of a helicon plasma source," *Rev. Sci. Instrum.*, vol. 81, no. 7, pp. 075 106-1–075 106-8, Jul. 2010.
[19] A. Fruchtman, "Neutral depletion in a collisionless plasmas," *IEEE Trans. Plasma Sci.*, vol. 36, no. 2, pp. 403–413, Apr. 2008.
[20] A. Fruchtman, "Energizing and depletion of neutrals by a collisional plasma," *Plasma Sources Sci. Technol.*, vol. 17, no. 2, pp. 024 016-1–024 016-10, May 2008.
[21] G. Makrinich and A. Fruchtman, "Experimental study of a radial plasma source," *Phys. Plasmas*, vol. 16, no. 4, pp. 043 507-1–043 507-8, Apr. 2009.
[22] G. Makrinich and A. Fruchtman, "Enhancement of electric force by ion–neutral collisions," *Appl. Phys. Lett.*, vol. 95, no. 18, pp. 181 504-1–181 504-3, Nov. 2009.
[23] M. A. Lieberman and A. J. Lichtenberg, *Principles of Plasma Discharges and Materials Processing*. New York: Wiley, 2005, ch. 3.
[24] A. Fruchtman, G. Makrinich, and J. Ashkenazy, "Two-dimensional equilibrium of a low temperature magnetized plasma," *Plasma Sources Sci. Technol.*, vol. 14, no. 1, pp. 152–167, Feb. 2005.
[25] K. D. Diamant, "Microwave cathode for air breathing electric propulsion," presented at the 31st Int. Electric Propulsion Conf., Ann Arbor, MI, Sep. 20–24, 2009, IEPC Paper 2009-015.

Amnon Fruchtman (SM'08) was born in Rehovot, Israel. He received the B.Sc. degree in physics from Tel Aviv University, Tel Aviv, Israel, in 1973 and the M.Sc. and Ph.D. degrees in physics from Hebrew University, Jerusalem, Israel, in 1976 and 1983, respectively.

After being a Postdoctoral Fellow with the Courant Institute of Mathematical Sciences, New York University, New York, he joined the Weizmann Institute of Science, Rehovot, where he left as an Associate Professor in 1995. He is currently a Professor with the Holon Institute of Technology, Holon, Israel. He spent sabbaticals at Princeton University, Princeton, NJ, in 1994–1995 and Ecole Polytechnique, Paris, France, in 2004. His areas of interest are free-electron lasers, high-power pulsed plasmas, helicon and other plasma sources, and electric propulsion.

Dr. Fruchtman is a Fellow of the American Physical Society.